HHS Public Access

Author manuscript

Biomaterials. Author manuscript; available in PMC 2019 September 09.

Published in final edited form as:

Biomaterials. 2019 February ; 192: 569–578. doi:10.1016/j.biomaterials.2018.11.036.

Engineering Hyaline Cartilage from Mesenchymal Stem Cells with Low Hypertrophy Potential via Modulation of Culture Conditions and Wnt/β-Catenin Pathway

Yuhao Deng[1,2,4], **Guanghua Lei**[1], **Zixuan Lin**[1,2], **Yuanheng Yang**[1,2,4], **Hang Lin**[2,3,*], **Rocky S. Tuan**[2,3,5,6,*]

[1.]Department of Orthopaedic Surgery, Xiangya Hospital, Central South University, Changsha, Hunan, China

[2.]Center for Cellular and Molecular Engineering, Department of Orthopaedic Surgery, University of Pittsburgh School of Medicine, Pittsburgh, PA 15219, USA

[3.]McGowan Institute for Regenerative Medicine, University of Pittsburgh School of Medicine, Pittsburgh, PA 15219, USA

[4.]Xiangya Third hospital, Central South University, Changsha, Hunan, China

[5.]Department of Bioengineering, University of Pittsburgh Swanson School of Engineering, PA, 15261, USA

[6.]The Chinese University of Hong Kong, Hong Kong, China

Abstract

Mesenchymal stem cells (MSCs) represent a promising cell source to regenerate articular cartilage, but current chondroinduction protocols, commonly using transforming growth factor-β (TGFβ), lead to concomitant chondrocytic hypertrophy with ossification risk. Here, we showed that a 14-day culture of MSCs-laden hyaluronic acid hydrogel in the presence of TGFβ, followed by 7 days culture in TGFβ-free medium, with the supplement of Wnt/β-catenin inhibitor XAV939 from day 10–21, resulted in significantly reduced hypertrophy phenotype. The stability of the hyaline phenotype of the MSC-derived cartilage, generated with a standard protocol (Control) or the optimized (Optimized) method developed in this study, was further examined through

[*]**Correspondence:** Rocky S. Tuan, PhD, Center for Cellular and Molecular Engineering, Department of Orthopaedic Surgery, University of Pittsburgh School of Medicine, Pittsburgh, PA, 15219, USA. rst13@pitt.edu, Fax: +1 4126245544, Tel: +1 4126242603, Hang Lin, PhD, Center for Cellular and Molecular Engineering, Department of Orthopaedic Surgery, University of Pittsburgh School of Medicine, Pittsburgh, PA, 15219, USA. hal46@pitt.edu, Fax: +1 4126245544, Tel: +1 4126245503.

Author Contributions

Y.D. contributed to the design of the experiments, collection and assembly of all data, data analysis and interpretation, and manuscript writing. G.L. performed data analysis and data interpretation, and provided financial support (Fellowship to support Y.D.). Y.Y. contributed to the real time PCR results in Figure 1 and 2, and the writing of the manuscript. Z.L. contributed to Figure S2B. H.L. conceived the idea, provided funding (Start-up fund), participated all data collection and analysis, and contributed majorly to manuscript writing. R.S.T. contributed to the data interpretation, manuscript writing and final approval of manuscript. R.S.T. also contributed financially (W81XWH-14-1-0217, 1UG3TR0021360 and 5R01EB019430).

Data Availability

The authors declare that all data supporting the findings of this study are available within the paper and its supplementary information, source data for the figures in this study are available from the authors upon request.

Competing Interests

The authors declare no competing interests.

intramuscular implantation in nude mice. After 4 weeks, constructs from Control group showed obvious mineralization; in contrast, the Optimized group displayed no signs of mineralization, and maintained cartilaginous histology. Further analysis showed that TGFβ treatment time affected p38 expression, while exposure to XAV939 significantly inhibited P-Smad 1/5 level, which together resulted in decreased level of Runx2. These findings suggest a novel treatment regimen to generate hyaline cartilage from human MSCs-loaded scaffolds, which have a minimal risk of eliciting endochondral ossification.

Keywords

MSC; Chondrogenesis; Hypertrophy; Wnt/β-catenin; Cartilage Tissue Engineering

1. INTRODUCTION

Due to the avascular nature of cartilage, focal cartilage defects (FCDs) have limited self-healing potential. Consequently, these defects will eventually contribute to premature development of osteoarthritis[1]. Current methods for the treatment of FCDs include cartilage transplantation, microfracture, and autologous chondrocyte implantation (ACI), but none of these are able to fully restore the structure and function of cartilage[2]. ACI has shown promising clinical outcomes, but it is limited by inherent disadvantages, such as donor-site morbidity and low availability of functional cells[3, 4].

Due to their relatively high abundance, chondrogenic differentiation capacity, and multi-passage expansion potential, adult mesenchymal stem cells (MSCs), in particular those derived from bone marrow (BMSCs), have emerged as an alternative cell source for cartilage repair [5]. Upon stimulation by chondrogenic factors, such as transforming growth factor-β (TGFβ), MSCs are able to express cartilage marker genes, including collagen type II (*COL2*) and aggrecan (*AGG*), and deposit proteoglycans containing sulfated glycosaminoglycans (GAGs)[2, 6]. In addition to traditional pellet or micromass culture, MSCs have also been combined with different biomaterial scaffolds for the purpose of cartilage tissue engineering. For example, we showed that MSCs encapsulated within novel hydrogels produced by visible light mediated photocrosslinking underwent robust chondrogenesis[7, 8]. Also, MSCs seeded in hyaluronic acid (HA) hydrogel showed superior production of collagen type II and chondroitin sulfate, but less collagen type I deposition, compared with other materials[9, 10]. With the addition of N-cadherin peptides, HA hydrogels enhanced early chondrogenesis of MSCs and cartilage-specific matrix production *in vivo* and *in vitro*[11]. Erickson et.al further showed that the macromer density of MSC-laden HA hydrogels could influence matrix deposition and mechanical property during MSC chondrogensis[12]. In all, HA is a good material that supports the chondrogenesis of MSC.

TGFβ is the most commonly used growth factor to initiate chondrogenic differentiation of MSCs[13], which however also causes a concomitant hypertrophic phenotype[14, 15]. Chondrocyte hypertrophy, a key step in endochondral ossification during bone development, is characterized by significant increase in cell volume and increased gene expression of collagen type X (*COL10*), alkaline phosphatase (*ALP*), and matrix metalloproteinase-13

(*MMP-13*)[3, 15, 16]. A recent study demonstrated a direct conversion of hypertrophic chondrocytes to osteoblasts, suggesting their bone-forming fate[17]. Currently, a number of strategies have been explored to reduce the level of hypertrophy in MSC-derived chondrocytes. For example, Hung et al. showed that hypoxia inhibited hypertrophy level in MSC-formed pellet cultures[18]. Kim et al. found that parathyroid hormone-related peptide (PTHrP) treatment decreased *COL10* gene expression in chondrogenically induced MSCs[19]. When being introduced after 14 days chondrogenesis, fibroblast growth factors-9 or 18 (FGF-9, 18) was shown to delay the appearance of hypertrophy-related changes[20]. Interestingly, our studies showed that transient exposure to TGFβ (such as 3 weeks) was sufficient to initiate MSC chondrogenesis and generate considerable deposition of cartilage matrix [21]. This provides us with the possibility of modifying TGFβ treatment profile to reduce hypertrophy, since the expression of hypertrophic genes increased with chondroinduction time[22].

In addition, specific pathways have been proposed to play major roles in the hypertrophy process[3]. For example, Erk is a potent regulator of chondrogenesis and osteogenesis[23–25]. Prasadam et al. showed that with the application of an Erk1/2 inhibitor, hypertrophic markers of articular cartilage chondrocytes decreased significantly[26]. Kim et al. further showed that upon application of an inhibitor of Erk1/2 from the 14th day after induction of chondrogenesis, gene expression of *COL2* increased and *COL10* decreased in hBMSCs[27], although the hypertrophy suppression effect is not robust. WNT signaling is another pathway involved in the regulation of chondrocyte hypertrophy. Janine et al. showed that blocking the Wnt/β-Catenin pathway antagonists, DKK1 and FRZB, led to more collagen type X deposition and mineralization in MSC pellet cultures[28]. Yang et.al found that temporal activation of Wnt pathway could enhance hypertrophy phenotype during MSC chondrogenesis[29]. Lietman et.al showed that Wnt inhibition attenuated type I collagen synthesis in human synovial fibroblasts[30]. Recent studies reported that lower *ALP* gene expression and less calcium deposition were detected with the inclusion of Wnt inhibitors in the chondroinductive medium[31, 32], but the underlying mechanism was not fully explored. Moreover, most of these studies were performed in traditional pellet culture conditions, which may not represent the actual application in clinic. For example, to treat cartilage defects, a scaffold is often needed to secure the transplanted cells in the defect site, which also serves as the template for cell differentiation and tissue regeneration. Therefore, whether the hypertrophy-suppression results generated from a pellet culture study are applicable to in-scaffold cultures remains unknown.

In this study, we aimed to generate minimally hypertrophic chondrocytes from hBMSCs that had been encapsulated within a chondrosupportive scaffold. We compared the chondrogenic ability and levels of hypertrophy of hBMSCs maintained under different culture conditions, including varying biomaterials for 3-dimensional (3D) culture, TGFβ treatment times, and supplement with a specific Erk1/2 inhibitor (PD98059)[33] or a Wnt inhibitor (XAV939)[34]. An optimal treatment profile that maximizes chondrogenesis and minimizes hypertrophy was then determined, and the ossification potential of hBMSC-derived cartilage was further tested by intramuscular implantation in immune compromised mice. Finally, we examined the involvement of specific signaling pathways.

2. MATERIALS AND METHODS

2.1 Human Bone Marrow Derived Mesenchymal Stem Cells (hBMSCs)

The isolation of hBMSCs from surgical human tissue specimens obtained from total joint arthroplasty was approved by the Institutional Review Boards (IRBs) of University of Pittsburgh and University of Washington. First, trabecular bone was cored out using a curette or rongeur, minced, rinsed, and cell obtained by sieving through 40-μm mesh screens to remove large tissue chunks. Cells were then pelleted by centrifugation (300g, 6 min). After rinsing, cells were re-suspended in MSC growth medium, containing GM (α-MEM containing 10% selected fetal bovine serum, FBS, Invitrogen, Carlsbad, CA), 1% antibiotics-antimycotics (Life Technologies, Carlsbad, CA), and 1.5 ng/ml fibroblast growth factor-2 (FGF-2) (RayBiotech, Norcross, GA)), and plated into 150 cm^2 tissue culture flasks. On day 4, cells were washed with phosphate-buffered saline (PBS) and fresh GM was added. The medium was changed every 3 to 4 days. Once 70 to 80% confluence was reached, cells were detached with 0.25% trypsin-EDTA (Life Technologies), placed in culture, and passaged. MSC populations isolated from individual patients were routinely validated as capable of osteogenic, adipogenic, and chondrogenic differentiation (data not shown). All hBMSCs used in the experiments were pooled cells obtained from 6 patients (57-year-old female, 60-year-old female, 48-year-old female, 62year-old male, 31-year-old male, and 19-year-old male), and used at passage 4.

2.2 Hyaluronic Acid (HA) Hydrogel Synthesis

Methacrylated HA (MeHA) macromer was synthesized by adding methacrylic anhydride (Sigma, St. Louis, MO) to HA solution (1% w/v, MW ~60 kDa, Lifecore, Chaska, MN), and incubated on ice overnight. The pH was adjusted regularly to 8.0, using 10 N NaOH. After extensive dialysis (3.5K MWCO) against deionized water, the MeHA preparation was lyophilized and stored dessicated before use. Lyophilized macromer preparation was dissolved in HBSS (HyClone, Logan, UT) at 2% (w/v) concentration, with 0.15% lithium phenyl-2,4,6-trimethylbenzoylphosphinate (LAP) added as the photoinitiator[7, 8].

2.3 In vitro chondrogenesis of hBMSCs in pellet and HA cultures

Pellet culture—Passage 4 MSCs at 90% confluency were trypsinized and pelleted. To make MSC pellet culture, cells were resuspended in full chondrogenic medium (CM: high-glucose Dulbecco's modified Eagle medium supplemented with 1% antibiotics-antimycotics, 0.1 μM dexamethasone (Sigma), 50 μg/mL ascorbate 2-phosphate (Sigma), 40 μg/mL L-proline (Sigma), 10 μg/mL ITS+ (Thermo Fisher, Waltham, MA), 10 ng/mL TGFβ3 (Peprotech, Rocky Hill, NJ)) at a concentration of 1×10^6 cells/mL. Aliquots (200 μL) containing 2×10^5 MSCs were pipetted into individual wells of conical-bottom 96-well plates (Thermo Fisher) and pelleted by centrifugation (300g, 10 min).

HA culture—Cells were suspended at a density of 20×10^6 cells/mL in a MeHA solution in HBSS (HyClone, Logan, UT) at 2% (w/v) concentration, with 0.15% lithium phenyl-2,4,6-trimethylbenzoylphosphinate (LAP) added as the photoinitiator which was synthesized as described by Fairbanks et al[35]. The cell/HA suspension was then transferred into a silicone

mold (5 mm diameter, 2 mm depth), and the hydrogel photocrosslinked by exposure to 395 nm light for 2 minutes [7].

Culture conditions—In Experiment 1 (Figure 1A), MSCs in pellet or HA constructs were cultured in CM for up to 28 days. Samples were collected at day 0, 7, 14, 21 and 28 (named as CM0, CM7, CM14, CM21, CM28) for analyses. In Experiment 2 (Figure 2A), MSCs in pellet or HA constructs were cultured in CM for 0, 7, 14, 21, or 28 days, then with basic chondrogenic medium (BM, same formula to CM but without TGFβ3) for an additional 7 days, named CM0BM7, CM7BM7, CM14BM7, CM21BM7, and CM28BM7. In Experiment 3, with the optimal culture conditions developed in experiments 1 and 2, Erk1/2 inhibitor (PD98059, 10 μM, Tocris, Minneapolis, MN) or Wnt inhibitor (XAV939,10 μM, Tocris) was added at various time points of the culture period to test their effects on the chondrocytic hypertrophy process during the chondrogenic program of MSCs.

2.4 RNA isolation and gene expression analysis

Total RNA was obtained by homogenizing all samples in Trizol Reagent (Invitrogen), following the protocol of the Rneasy Plus Mini Kit (QIAGEN, Germantown, MD, USA), and quantified spectroscopically using a Nanodrop 2000c Spectrophotometer (Thermo Fisher). Reverse transcription was performed using SuperScript™ IV VILO™ Master Mix (Invitrogen), and polymerase chain reaction (PCR) was performed on an Applied Biosystems real-time PCR system using SYBR Green Reaction Mix (Applied Biosystems, Foster City, CA, USA). Transcript levels of typical chondrogenic and hypertrophic genes, including *COL2, AGG, COL10, MMP-13, and ALP*, were analyzed, with values normalized to that of the housekeeping gene, ribosomal protein L13a (RPL13a). Collagen I (*COL1*) gene expression was analyzed with values normalized to 18S rRNA as housekeeping gene. Relative gene expression was calculated using the $^{\Delta\Delta}$Ct method. The sequences of primers for each gene are listed in supplementary Table 1 (Table S1).

2.5 Biochemical analyses

hBMSC cultures were homogenized and digested in papain solution (125 μg/ml papain, 50 mM sodium phosphate buffer, 2 mM N-acetyl cysteine (Sigma), pH=6.5), and incubated overnight at 60°C. Each construct (around 40–50 μL) was treated with 300 μl of papain buffer. Afterwards, the suspension was cleared by centrifugation (12,000g, 15 min) and the supernatant was collected. For GAG analysis, the 1,9-dimethylmethylene blue dye-binding assay (Blyscan, Biocolor, United Kingdom) was used using a standard curve derived from chondroitin-6-sulfate. DNA content was measured using the Picogreen dsDNA assay (Molecular Probes, Tarrytown, NY).

2.6 Histology, Immunohistochemistry and Immunofluorescence

All samples were fixed in 10% paraformaldehyde, dehydrated using a graded ethanol series, embedded in paraffin, and sectioned at a thickness of 6 μm following a standard histological procedure. Sections were stained with Safranin O/Fast Green (Millipore Sigma, Burlington, MA) or Alizarin Red (Rowley Biochemical, Danvers, MA). Alkaline phosphatase activity was determined histochemically using a commercial reagent kit (Sigma). For immunohistochemistry (IHC), deparaffinized and rehydrated sections were incubated with

primary antibodies against human collagen type II, collagen type X, and osteocalcin (Abcam, Cambridge, MA) at 4°C overnight, followed by incubation with appropriate secondary antibodies. Immunostaining was carried out using the Vectastain ABC kit and NovaRED peroxidase substrate kit (Vector Labs, Burlingame, CA, USA), and images were acquired with the OLYMPUS CKX41 microscope and staining intensities quantified with NIH Image-J software. For immunofluorescence (IF), primary antibodies against human collagen type I and CD31 (Abcam) were used to incubate sections at 4°C overnight, followed by incubation with appropriate secondary antibodies. Vectashield Mounting Medium with DAPI (Vector Labs) was used to stain nuclei. Images were acquired with Olympus IX2-USB microscope.

2.7 Western blot analysis

Samples were homogenized in RIPA buffer (Sigma) and supplemented with protease and phosphatase inhibitors (ThermoFisher). Proteins were fractionated electrophoretically on NuPAGE™ 4–12% Bis-Tris Gel (Invitrogen) and then transferred to a polyvinylidene fluoride (PVDF) membrane using the iBlot Dry Blotting System (Invitrogen). Primary antibodies directed against glyceraldehyde-3-phosphate dehydrogenase (GAPDH), total Erk1/2, phosphorylated Erk1/2 (P-Erk1/2), β-catenin, p38, phosphorylated p38 (P-p38), Smad1, phosphorylated Smad1/5 (P-Smad1/5), Runx2, Smad2/3, phosphorylated Smad2/3 (P-Smad2/3), were purchased from Cell Signaling Technology (Danvers, MA, USA). Antibodies against phosphorylated Smad2 (P-Smad2) were purchased from ThermoFisher company. Bound primary antibodies were detected using horseradish peroxidase (HRP)-linked secondary antibodies (GE Healthcare Life Sciences, Malborough, MA, USA) and SuperSignal™ West Dura Extended Duration Substrate (ThermoFisher). Images were acquired by ChemiDocTM Touch Imaging System (BIO-RAD, Hercules, CA, USA) and quantified with the NIH Image-J software.

2.8 *In vivo* intramuscular implantation in SCID mice

The animal study was performed with the approval of the University of Pittsburgh Institutional Animal Care and Use Committee, and all guideline requirements were followed in all animal procedures. Severe Combined Immunodeficiency mice (SCID, B6.CB17-Prkdc^{scid}/SzJ, male, 8–12 weeks old) were purchased from The Jackson Laboratory (Bar Harbor, ME). Intramuscular implantation sites were prepared on the thigh muscles of SCID mice. Bilateral implantation was performed after the mice were anesthetized with 2% to 3% isoflurane and maintained in a surgical plane during the procedure with 1.5% isoflurane. In this study, two groups were used, including control and optimized groups. hBMSC-laden HA constructs were fabricated as described above and cultured in chondrogenic medium before being implanted. The group consisting of hBMSC-seeded HA constructs that were cultured in CM for 21 days was designated as the Control group representing conventional production of engineered cartilage. The Optimized group involved hBMSC-seeded HA scaffolds that were cultured under conditions optimized in this study. The Control and Optimized groups each consisted of 4 mice. After 4 weeks, the mice were sacrificed, and HA constructs were collected for micro-CT analysis and histology.

2.9 Micro-CT analysis

After *in vivo* implantation for 4 weeks, mice were sacrificed for micro-CT (Scanco Medical vivaCT 40, Switzerland) analysis to detect bone formation. Scans were acquired at 45 kVp, 88 μA, 300 ms integration time and at an isotropic voxel size of 35 μm. Raw micro-CT images from the scans were converted into 3D reconstructions.

2.10 Statistical analysis

Statistical analysis was performed by one-way and two-way analysis of variance (ANOVA) or two-tailed *t*-tests using GraphPad Prism7 (GraphPad Software, San Diego, CA, USA). For multiple comparisons between groups, p values < 0.05 were considered statistically significant.

3. RESULTS

3.1 Culture in HA reduces hypertrophic phenotype

As mentioned above, a biomaterial scaffold is often necessary for cartilage regeneration. Therefore, in this study, we first compared the hypertrophy level of chondroinduced hBMSCs in the four commonly used biomaterials for cartilage regeneration, including alginate, gelatin, agarose, and HA, specifically respect to the expression ratio of collagen type II *to* type X (*COL2/COL10*) as the indicator. As shown in Supplementary Figure 1 (Figure S1), our results showed that hBMSCs within HA displayed the highest *COL2/COL10* ratio. Therefore, HA was chosen for the 3D culture system in the following studies.

To further characterize the profiles of chondrogenic and hypertrophic gene expression during chondroinduction, hBMSCs were encapsulated in HA scaffolds and the cultured constructs collected and analyzed at various time points, and compared to standard pellet culture as control (Figure 1A). The results in Figure 1B showed that maximal *COL2* and *AGG* expression in hBMSCs cultured within an HA scaffold appeared at day 21. In contrast, expression of these two genes in MSCs in pellet culture reached plateau values at day 14, which were lower than those in HA culture. Interestingly, as analyzed by Western blotting, P-Smad 2/3 levels, a signaling activating chondrogenesis, appeared earlier at a higher level in HA cultures *versus* pellet cultures (Figure S2A), suggesting a possible functional correlation. We also monitored cell proliferation capacity in pellet and HA culture by using Picogreen dsDNA assay (Figure S2B). Cells in both pellet and HA proliferated during 28 days culture, but the cells in pellet culture displayed a higher proliferation rate than those in HA culture. Interestingly, significantly higher *COL2/10* values in the HA culture, compared to pellet culture, were observed at days 14, 21, and 28, resulting primarily from higher *COL2* expression levels. Moreover, the level of *ALP* expression was significantly lower in the HA cultures than in pellet cultures (Figure 1B), which was further confirmed by ALP activity staining (Figure 1C). However, as shown in Figure S3, COL10 protein was still detectable in HA culture, suggesting the need for further optimization of the culture system.

3.2 Optimized TGFβ exposure time reduces hypertrophy

We next explored whether the hypertrophy program of MSC-derived chondrocytes could also be affected by TGFβ treatment time, a topic which had not been investigated previously.

As shown in Figure S4, chondrogenesis of HA-encapsulated hBMSCs was seen to persist for several additional days after removal of TGFβ from the culture medium. Surprisingly, this residual effect of TGFβ also resulted in a hypertrophy-inhibiting outcome (Figure S4). Therefore, in this study, all of the hBMSC constructs were subjected to an additional 7-day period of post-TGFβ culture in basic medium without TGFβ (BM), after having been treated with full chondrogenic medium (CM) for different lengths of time (Figure 2A).

As shown in Figure 2B, under the new culture regimen of truncated TGF-β treatment, we observed a significant decrease in *COL10* expression in HA culture, compared to pellet culture, which was not seen in the traditional culture condition with continuous TGFβ exposure (Figure 1B). Of particular significance, the highest *COL2/COL10* ratio was achieved by first culturing hBMSCs in HA in CM for 14 days, followed by 7 days in BM (group CM14BM7, Figure 2B&C).

3.3 XAV939 treatment lowers expression of hypertrophy genes

The Wnt/β-catenin and Erk1/2 signaling pathways are known to regulate mesenchymal chondrogenesis and chondrocyte hypertrophy[31, 36]. To assess whether these signaling pathways could be exploited to further enhance the hyaline chondrocyte phenotype in our HA-encapsulated hBMSC cultures, we supplemented PD98059 (an Erk1/2 pathway inhibitor) or XAV939 (a Wnt pathway inhibitor) into culture medium. The effectiveness of the agents as inhibitors of signaling was first assessed by Western blotting, which showed that phosphorylated Erk1/2 or β-catenin (a component of WNT signaling pathway) was inhibited, respectively, after PD98059 or XAV939 was introduced into the culture medium (Figure 3A and 3B). Our initial data also showed that early treatment with these inhibitors from day 0 or 5 adversely affected chondrogenesis (data not shown). Therefore, in this study, all tested inhibitors were introduced at day 10, 14, or 17, and cultured with constructs until day 21, using the optimized condition (CM14BM7). As shown in Figure 3C, we did not observe a difference in gene expression profiles between the control group (Ctrl) and all PD98059 treated groups, indicating that modulating the Erk1/2 pathway might not affect hypertrophy in our special culture conditions.

Interestingly, in the XAV939-treated group, *COL10* and *ALP* expression levels were lower than those control group, in particular when XAV939 treatment was applied from day 10 to day 21. The ratio of *COL2/COL10* expression was also significantly higher (Figure 3C). In addition, the reduction in *COL10* expression was accompanied by significantly reduced deposition of collagen type X protein (Figure 3D-vi). More importantly, treatment with XAV939 did not compromise the levels of P-Smad2/3 (Figure S5B), chondrogenic gene expression (Figure 3C), or the production of GAG (Figure 3D-i-iv).

In summary, supplementation of XAV939 treatment (days 10–21) to the CM14BM7 group of HA-encapsulated hBMSC constructs represents the best culture condition to generate minimally hypertrophic chondrocytes from hBMSCs, which was designated as the “Optimized” group in the following studies. The CM21 group without XAV939, representing the conventional chondroinduction method, was used as the “Control” group. As shown in Figure 4A, no significant change was found in these two groups with reference to *COL2* and *AGG* (Figure 4A). Histological results showed comparable GAG (Figure 4B-i

& ii) and collagen type II deposition in the Control and Optimized groups (Figure 4B- iii & iv, D). The GAG/dsDNA measurement further confirmed similar level of chondrogenesis in these two groups (Figure 4C). However, compared to the Control group, the Optimized group displayed significantly reduced hypertrophic gene expression (Figure 4A) and collagen type X deposition (Figure 4B- v & vi, E).

We also examined the gene expression and deposition of collage type I (COL1), which is not presence in healthy hyaline cartilage. In addition, it is a critical component for bone formation. Therefore, a low level of COL1 is desired for articular cartilage regeneration. Interestingly, comparing to those in Control group, cells in Optimized group displayed significantly lower *COL1* expression (Figure 5A), and produced much less COL1 protein, revealed by immunofluorescence (Figure 5B), suggesting the robust potential of XAV939 in suppressing the generation of COL1.

Taken together, these results indicated that cells in the Optimized group displayed comparable chondrogenic phenotype, but a low hypertrophic and osteogenic phenotype, compared to those in the Control group.

3.4 Optimally chondroinduced hBMSCs don't undergo ossification

As chondrocyte hypertrophy is a precursor to endochondral ossification *in vivo*, accompanied by matrix mineralization[17], we would like to test whether hBMSCs-derived cartilage, generated under the culture conditions optimized as described above, could retain their hyaline, non-hypertrophic phenotype when implanted *in vivo*. Intramuscular implantation is the most commonly used method to observe ectopic bone formation, and was thus employed in our study. Before implantation, both the Control and Optimized groups were analyzed by Western blot to assess their potential for osteogenesis. As shown in Figure 6A, constructs from the Optimized group had lower phosphorylated Smad1/5, phosphorylated p38, and Runx2 protein levels.

Engineered constructs were implanted into the thigh muscle pockets in mice (Figure 6B). After 4 weeks, micro-CT analysis showed ectopic bone formation only in the implantation site of constructs from the Control group (Figures 6C and 6D). In the samples from Control group, invasion of endothelial cells was observed (Figure S6), suggesting the initiation of angiogenesis. Histological analysis of the implantation site tissue also showed Alizarin Red positive staining and immunopositive osteocalcin staining only in the Control group (Figure 6E-i & ii). There results clearly demonstrated that hBMSCs-derived cartilage, using traditional chondroinduction condition, possessed high bone formation potential. While in the samples from Optimized group, no obvious bone formation was observed based on the results from all analysis methods (Figure 6C-ii, E-iv & v). In addition, safranin O staining showed denser and more uniform GAG staining in the Optimized group than in the Control group (Figure 6E- iii & vi), suggesting the preservation of the cartilage phenotype.

3.5 Pathway involved in XAV939 suppression of hypertrophy

The nature of the potential mechanism underlying hypertrophy suppression in our optimized culture system was next explored. This was carried out by examining the influence on key signaling pathways by Western blotting of samples from 4 groups: (1) CM0; (2) CM21

without XAV939 treatment; (3) CM14BM7 without XAV939 treatment; and (4) CM14BM7 with XAV939 treatment (Figure 7A). By comparing groups CM21 and CM14BM7, we found that truncation of TGFβ treatment resulted in significant reduction of the levels of P-Smad1/5 and p38, two known regulators of Runx2, although the level of Runx2 level of only slightly reduced. On the other hand, by comparing the CM14BM7 groups with or without XAV939 treatment, we saw a significantly decreased level of P-Smad1/5 and Runx2, but not P-p38. This result was observed in other independent tests (such as Figure S5A).

4. DISCUSSION

Our findings represent a novel method of inducing chondrogenesis with a minimal hypertrophic potential in human MSCs, which may be applicable to the clinical repair of joint cartilage defects. The conclusion from this mechanistic study also represents a significant advance in understanding the chondrocytic hypertrophy of MSCs.

In this study, we first assessed the influence of TGFβ treatment time on chondrogenesis and hypertrophy. In a previous study using pellet culture [22], peak levels of *COL2*, *AGG and ALP* were found at around day 14 after TGFβ stimulation, which agreed with our results in Figure 1B. However, the expression of *COL10* and *MMP13* displayed a continuous increase up to 21 days in their study, while our results showed a peak at day 7 or 14. This difference could be due to the different types of TGFβ that were used (TGFβ1 in the study by Handorf et al. [22] and TGFβ3 in ours). In fact, TGFβ1 was shown to result in higher hypertrophic gene expression in mouse suture-derived mesenchymal cells [37]. In summary, these findings showed that changing TGFβ treatment time was not beneficial in terms of the production of chondrocytes of low hypertrophic potential.

Therefore, we next tested the effect of placing hBMSCs in additional culture in BM after the establishment of the chondrogenesis program. The rationale behind this was that our previous study showed that MSCs could maintain a chondrocyte-like phenotype in BM without TGFβ for up to 4 weeks after they were treated with TGFβ for 3 weeks[21]. Since TGFβ appears to drive hypertrophy, we examined whether additional maintenance in BM, after the establishment of chondrogenesis, was able to mitigate the emergence of the hypertrophic phenotype without sacrificing the chondrogenic phenotype. As shown in Figure 2, after 2 weeks of chondroinduction, an additional 7 days of BM culture significantly reduced the expression of *COL10* without affecting *COL2* or *AGG* expression. When a longer culture time of up to 14 days was tested, detectable decrease of *COL2* and *AGG* expression was seen (data not shown).

With the optimized culture conditions, we successfully suppressed the expression of hypertrophy genes and deposition of collagen type X. However, the levels of osteogenesis-associated factors, such as P-Smad 1/5 and Runx2, were still high (Figure 7A), suggesting that the potential of an endochondral ossification event remained, particularly upon appropriate stimulation. We thus sought additional hypertrophy-inhibiting methods by directly targeting key signaling pathways. Previously, when Erk1/2 inhibitor, PD98059, was introduced into the culture medium after 14 days, chondrogenesis gene expression was increased while hypertrophy gene expression was slightly decreased[27]. This result are in

agreement with the known hypertrophy-suppressing effects of FGF-9 and FGF-18, which function through the FGF receptor 3 (FGFR3) and mitogen activated protein kinase (MAPK) pathway including Erk1/2[38]. However, it should be noteworthy that, under our culture conditions, we did not observe a major effect of PD98059, consistent with the known complex functional involvement of the Erk1/2 pathway in chondrogenesis and hypertrophy.

The Wnt/β-Catenin pathway is another important regulator of hypertrophy, but its exact involvement remains controversial. Blockade of the WNT pathway antagonists, DKK1 and FRZB, has been found to lead to more collagen type X deposition and matrix mineralization[28]. A recent study using pellet culture showed that inhibition of WNT signaling during differentiation prevented calcification and maintained cartilage properties[31]. These findings suggest that WNT signaling promotes the hypertrophy process. However, Yang et al. found that co-activation of TGF signaling pathway with β-catenin led to lower osteogenic potential[29], indicating an opposite function of WNT. Our results (Figures 3, 4) support the hypertrophy-promoting role of WNT signaling. Specifically, we observed that XAV939 treatment inhibited the expression of all hypertrophy genes tested, including *COL10*, *MMP-13*, and *ALP*. In a recent study using another WNT inhibitor (IWP-2), the hypertrophy-suppressing effect was observed under specific culture conditions with pre-activation of the WNT pathway[31]. Such differences may be due to the different mechanisms of these WNT inhibitors (tankyrase for XAV939 and porcupine for IWP-2), and different culture conditions being used. Interestingly, we also observed robust effect of XAV 939 in suppressing collagen type I expression (Figure 5), which suggests its dual function in reducing chondrocytic hypertrophy and fibrosis. In fact, WNT inhibitors have been shown to inhibit COL1 expression in fibroblasts[39].

For the *in vivo* study (Figure 6), we collected all samples after 4 weeks post-implantation. This sampling time has also been used in other studies [11, 40, 41]. From the macro-appearance, all the constructs maintained original cylindrical structures. Such low degradation rate of HA hydrogel also was reported from other studies[42, 43]. However, we noticed that there were GAG-free zones in the constructs from Control group (Figure 6), which were coincided with the OCN positive area. Therefore, an active transition from cartilage to bone was ongoing in the constructs from Control group.

Lastly, we examined the underlying signaling mechanisms responsible for the hypertrophy suppression effects observed here. Specifically, we focused on known pathways that regulate osteogenesis, which usually follows hypertrophy. We focused on Smad1/5 and p38, since they lead to Runx2 phosphorylation and osteogenesis[44, 45]. We observed high levels of P-Smad1/5 and Runx2 in naïve MSCs(Figure 7A), strongly indicating an intrinsic osteogenic potential [3, 46, 47]. After 21 days culture in chondrogenic medium, P-Smad1/5 level slightly decreased due to the lack of osteoinductive molecules in the medium (BMP, etc.). However, the expression of Runx2 was increased, which was the consequent of TGF-β treatment[45, 48]. We did not observe an increase in P-p38 with chondrogenesis[49], which may be associated with the absence of serum in the chondrogenic medium[50].

Our results in Figures 4–7 showed that the WNT pathway promoted or maintained the TGFβ-Smad1/5-Runx2 pathway, and its inhibition prevented chondrocyte hypertrophy as

well as terminal ossification, in agreement with the findings of Hellingman et al.[44]. Interestingly, as show in Figures 7A, P-p38 level slightly increased after XAV939 treatment, suggesting a weak crosstalk between the p38 and WNT pathways [51]. However, such an increase in P-p38 after XAV 939 treatment did not accompany the enhancement of Runx2 levels. In contrast, Runx2 level was actually suppressed after XAV939 treatment. In other words, increased P-p38 likely enhances Runx2 expression, which however is overwhelmed by the opposite effect of the inhibition of P-Smad1/5. Therefore, we propose that p38 participates in chondrocyte hypertrophy and the subsequent ossification process[52], but its effect is minor in comparison with that of the Wnt/β-catenin-Smad1/5 pathway. Interestingly, Kim et al. also reported that direct inhibition of p38 with SB203580 actually promoted the expression of *COL10* in chondrogenic hMSCs, if SB203580 was introduced after 14 days chondrogenesis[27]. Interestingly, the combination of BMP-2 and TGF-β lead to amplified expression of hypertrophy markers, including ALP and COL10[53]. Similar to our results, Occhetta et.al. showed that inhibition of BMP-Smad1/5/9 pathway further inhibited hypertrophy profile in MSC-derived chondrocyte in a dose-dependent pattern [54]. These results indicated the potential crosstalk between Wnt pathway and BMP pathway, which needs be further studied in the future.

Taken together, we proposed a mechanism of how our treatment method suppressed the hypertrophy/osteogenesis (Figure 7B) of hBMSCs-loaded HA. When TGFβ bound to its chondrogenic receptors Activin receptor-like kinase (ALK)-1, both the Smad1/5 and p38 pathways were activated as well, which together activated Runx2 transcription. Tentative removal of TGFβ from the medium slightly inhibited Smad1/5, p38, and Runx2. In contrast, inhibition of Wnt/β-Catenin with XAV939 completely blocked the phosphorylation of Smad1/5 and significantly decreased the level of Runx2. Based on our results, the Tankyrase/β-catenin-Smad1/5-Runx2 pathway is suggested to play a major role in regulating the hypertrophy process. p38 may also participate in this process, but its effect is considered as minor.

Our hypertrophy-suppressing culture conditions may be expanded to other bioscaffolds in the future. For example, sulfated HA, produced by conjugating sulfate groups to HA, has shown enhanced chondrogenesis and reduced hypertrophy of hMSCs in comparison with naïve HA[55]. In addition, long-term stability and reparative effect of hMSC-derived chondrocytes require further investigation using animal model or other methods. Recently, Somoza et al. performed a microarray analysis on human neonatal articular cartilage and established a method to molecularly define articular cartilage[56]. We will perform a similar analysis to compare the transcriptomic profiles of native and MSCs-derived chondrocytes.

5. Conclusion

Here, we developed a novel treatment approach, a combination of modifying culture conditions and modulating the Wnt/Catenin pathway, to inhibit spontaneous chondrocytic hypertrophy during human MSC chondrogenesis, without the introduction of additional hypertrophy-inducing conditions, such as hypertrophic medium or pre-activation of Wnt signaling. In particular, we showed that group CM14BM7 (14 days TGF-β stimulation with an additional 7 days of culture without TGF-β) represents an optimal culture condition to

induce chondrogenesis and inhibit hypertrophy. In addition, XAV939 was an effective inhibitor of the Wnt/β-catenin pathway, and was able to further suppress hypertrophy and prevent bone formation *in vivo*. We also showed that TGF-β treatment time affected p38 expression and XAV939 significantly inhibited the Smad 1/5 level, which together led to decreased expression of Runx2. Our findings represent a novel method of inducing chondrogenesis with a reduced hypertrophic potential in human MSCs, which may be applicable to the clinical repair of joint cartilage defects. The conclusion from this mechanistic study also represents a significant advance in understanding the chondrocytic hypertrophy of MSCs.

Supplementary Material

Refer to Web version on PubMed Central for supplementary material.

Acknowledgment

The authors thank Dr. Paul Manner (University of Washington) for generously providing human tissue, Dr. Jian Tan (University of Pittsburgh) for isolating hBMSCs, Dr. Bing Wang (University of Pittsburgh) for performing animal surgery, Dr. HongShuai Li (University of Pittsburgh) for the training in micro-CT, and Dr. Peter Mittwede (University of Pittsburgh Medical Center) for manuscript editing. This work was supported by the Department of Defense (W81XWH-14-1-0217), National Institutes of Health (1UG3TR0021360 and 5R01EB019430), and Dr. Hang Lin's Start-up fund (University of Pittsburgh). Yuhao Deng and Yuanheng Yang thank the Third Xiangya Hospital of Central South University for research fellowship support.

References

[1]. Magnussen RA, Dunn WR, Carey JL, Spindler KP, Treatment of Focal Articular Cartilage Defects in the Knee, Clinical Orthopaedics and Related Research 466(4) (2008) 952–962. [PubMed: 18196358]

[2]. Chen FH, Rousche KT, Tuan RS, Technology Insight: adult stem cells in cartilage regeneration and tissue engineering, Nat Clin Pract Rheumatol 2(7) (2006) 373–82. [PubMed: 16932723]

[3]. Chen S, Fu P, Cong R, Wu H, Pei M, Strategies to minimize hypertrophy in cartilage engineering and regeneration, Genes Dis 2(1) (2015) 76–95. [PubMed: 26000333]

[4]. Kon E, Filardo G, Di Matteo B, Perdisa F, Marcacci M, Matrix assisted autologous chondrocyte transplantation for cartilage treatment, Bone and Joint Research 2(2) (2013) 18–25. [PubMed: 23610698]

[5]. Bian L, Zhai DY, Mauck RL, Burdick JA, Coculture of human mesenchymal stem cells and articular chondrocytes reduces hypertrophy and enhances functional properties of engineered cartilage, Tissue Eng Part A 17(7–8) (2011) 1137–45. [PubMed: 21142648]

[6]. Noth U, Steinert AF, Tuan RS, Technology insight: adult mesenchymal stem cells for osteoarthritis therapy, Nat Clin Pract Rheumatol 4(7) (2008) 371–80. [PubMed: 18477997]

[7]. Sun AX, Lin H, Fritch MR, Shen H, Alexander PG, DeHart M, Tuan RS, Chondrogenesis of human bone marrow mesenchymal stem cells in 3-dimensional, photocrosslinked hydrogel constructs: Effect of cell seeding density and material stiffness, Acta biomaterialia 58 (2017) 302–311. [PubMed: 28611002]

[8]. Lin H, Cheng AW, Alexander PG, Beck AM, Tuan RS, Cartilage tissue engineering application of injectable gelatin hydrogel with in situ visible-light-activated gelation capability in both air and aqueous solution, Tissue Eng Part A 20(17–18) (2014) 2402–11. [PubMed: 24575844]

[9]. Chung C, Burdick JA, Influence of three-dimensional hyaluronic acid microenvironments on mesenchymal stem cell chondrogenesis, Tissue Engineering Part A 15(2) (2008) 243–254.

[10]. Erickson IE, Kestle SR, Zellars KH, Farrell MJ, Kim M, Burdick JA, Mauck RL, High mesenchymal stem cell seeding densities in hyaluronic acid hydrogels produce engineered cartilage with native tissue properties, Acta Biomater 8(8) (2012) 3027–34. [PubMed: 22546516]

[11]. Bian L, Guvendiren M, Mauck RL, Burdick JA, Hydrogels that mimic developmentally relevant matrix and N-cadherin interactions enhance MSC chondrogenesis, Proceedings of the National Academy of Sciences 110(25) (2013) 10117–10122.

[12]. Erickson IE, Huang AH, Sengupta S, Kestle S, Burdick JA, Mauck RL, Macromer density influences mesenchymal stem cell chondrogenesis and maturation in photocrosslinked hyaluronic acid hydrogels, Osteoarthritis and Cartilage 17(12) (2009) 1639–1648. [PubMed: 19631307]

[13]. Yoo JU, Barthel TS, Nishimura K, Solchaga L, Caplan AI, Goldberg VM, Johnstone B, The chondrogenic potential of human bone-marrow-derived mesenchymal progenitor cells, J Bone Joint Surg Am 80(12) (1998) 1745–57. [PubMed: 9875932]

[14]. Dexheimer V, Gabler J, Bomans K, Sims T, Omlor G, Richter W, Differential expression of TGF-β superfamily members and role of Smad1/5/9-signalling in chondral versus endochondral chondrocyte differentiation, Scientific reports 6 (2016) 36655. [PubMed: 27848974]

[15]. Somoza RA, Welter JF, Correa D, Caplan AI, Chondrogenic differentiation of mesenchymal stem cells: challenges and unfulfilled expectations, Tissue Eng Part B Rev 20(6) (2014) 596–608. [PubMed: 24749845]

[16]. Mueller MB, Tuan RS, Functional characterization of hypertrophy in chondrogenesis of human mesenchymal stem cells, Arthritis & Rheumatology 58(5) (2008) 1377–1388.

[17]. Yang L, Tsang KY, Tang HC, Chan D, Cheah KS, Hypertrophic chondrocytes can become osteoblasts and osteocytes in endochondral bone formation, Proceedings of the National Academy of Sciences 111(33) (2014) 12097–12102.

[18]. Lee HH, Chang CC, Shieh MJ, Wang JP, Chen YT, Young TH, Hung SC, Hypoxia enhances chondrogenesis and prevents terminal differentiation through PI3K/Akt/FoxO dependent anti-apoptotic effect, Sci Rep 3 (2013) 2683. [PubMed: 24042188]

[19]. Kim Y-J, Kim H-J, Im G-I, PTHrP promotes chondrogenesis and suppresses hypertrophy from both bone marrow-derived and adipose tissue-derived MSCs, Biochemical and biophysical research communications 373(1) (2008) 104–108. [PubMed: 18554504]

[20]. Correa D, Somoza RA, Lin P, Greenberg S, Rom E, Duesler L, Welter JF, Yayon A, Caplan AI, Sequential exposure to fibroblast growth factors (FGF) 2, 9 and 18 enhances hMSC chondrogenic differentiation, Osteoarthritis Cartilage 23(3) (2015) 443–53. [PubMed: 25464167]

[21]. Huang AH, Stein A, Tuan RS, Mauck RL, Transient exposure to transforming growth factor beta 3 improves the mechanical properties of mesenchymal stem cell–laden cartilage constructs in a density-dependent manner, Tissue Engineering Part A 15(11) (2009) 3461–3472. [PubMed: 19432533]

[22]. Handorf AM, Chamberlain CS, Li W-J, Endogenously produced Indian Hedgehog regulates TGFβ-driven chondrogenesis of human bone marrow stromal/stem cells, Stem cells and development 24(8) (2014) 995–1007.

[23]. Wortzel I, Seger R, The ERK cascade: distinct functions within various subcellular organelles, Genes & cancer 2(3) (2011) 195–209. [PubMed: 21779493]

[24]. Boulton TG, Cobb MH, Identification of multiple extracellular signal-regulated kinases (ERKs) with antipeptide antibodies, Cell regulation 2(5) (1991) 357–371. [PubMed: 1654126]

[25]. Pittenger MF, Mackay AM, Beck SC, Jaiswal RK, Douglas R, Mosca JD, Moorman MA, Simonetti DW, Craig S, Marshak DR, Multilineage potential of adult human mesenchymal stem cells, science 284(5411) (1999) 143–147. [PubMed: 10102814]

[26]. Prasadam I, van Gennip S, Friis T, Shi W, Crawford R, Xiao Y, ERK-1/2 and p38 in the regulation of hypertrophic changes of normal articular cartilage chondrocytes induced by osteoarthritic subchondral osteoblasts, Arthritis Rheum 62(5) (2010) 1349–60. [PubMed: 20155832]

[27]. Kim H-J, Im G-I, The Effects of ERK1/2 Inhibitor on the Chondrogenesis of Bone Marrow–and Adipose Tissue–Derived Multipotent Mesenchymal Stromal Cells, Tissue Engineering Part A 16(3) (2009) 851–860.

[28]. Zhong L, Huang X, Rodrigues ED, Leijten JC, Verrips T, El Khattabi M, Karperien M, Post JN, Endogenous DKK1 andFRZB Regulate Chondrogenesis and Hypertrophy in Three-Dimensional Cultures of Human Chondrocytes and Human Mesenchymal Stem Cells, Stem cells and development 25(23) (2016) 1808–1817. [PubMed: 27733096]

[29]. Yang Z, Zou Y, Guo XM, Tan HS, Denslin V, Yeow CH, Ren XF, Liu TM, Hui JH, Lee EH, Temporal activation of β-catenin signaling in the chondrogenic process of mesenchymal stem cells affects the phenotype of the cartilage generated, Stem cells and development 21(11) (2011) 1966–1976.

[30]. Lietman C, Wu B, Lechner S, Shinar A, Sehgal M, Rossomacha E, Datta P, Sharma A, Gandhi R, Kapoor M, Inhibition of Wnt/β-catenin signaling ameliorates osteoarthritis in a murine model of experimental osteoarthritis, JCI insight 3(3) (2018).

[31]. Narcisi R, Cleary MA, Brama PA, Hoogduijn MJ, Tüysüz N, ten Berge D, van Osch GJ, Long-term expansion, enhanced chondrogenic potential, and suppression of endochondral ossification of adult human MSCs via WNT signaling modulation, Stem cell reports 4(3) (2015) 459–472. [PubMed: 25733021]

[32]. Embree MC, Chen M, Pylawka S, Kong D, Iwaoka GM, Kalajzic I, Yao H, Shi C, Sun D, Sheu TJ, Koslovsky DA, Koch A, Mao JJ, Exploiting endogenous fibrocartilage stem cells to regenerate cartilage and repair joint injury, Nat Commun 7 (2016) 13073. [PubMed: 27721375]

[33]. Seghatoleslami MR, Roman-Blas JA, Rainville AM, Modaressi R, Danielson KG, Tuan RS, Progression of chondrogenesis in C3H10T1/2 cells is associated with prolonged and tight regulation of ERK1/2, Journal of cellular biochemistry 88(6) (2003) 1129–1144. [PubMed: 12647296]

[34]. Martino MM, Maruyama K, Kuhn GA, Satoh T, Takeuchi O, Müller R, Akira S, Inhibition of IL-1R1/MyD88 signalling promotes mesenchymal stem cell-driven tissue regeneration, Nature communications 7 (2016).

[35]. Fairbanks BD, Schwartz MP, Bowman CN, Anseth KS, Photoinitiated polymerization of PEG-diacrylate with lithium phenyl-2, 4, 6-trimethylbenzoylphosphinate: polymerization rate and cytocompatibility, Biomaterials 30(35) (2009) 6702–6707. [PubMed: 19783300]

[36]. Bobick BE, Matsche AI, Chen FH, Tuan RS, The ERK5 and ERK1/2 signaling pathways play opposing regulatory roles during chondrogenesis of adult human bone marrow-derived multipotent progenitor cells, Journal of cellular physiology 224(1) (2010) 178–186. [PubMed: 20232315]

[37]. James AW, Xu Y, Lee JK, Wang R, Longaker MT, Differential effects of TGF-beta1 and TGF-beta3 on chondrogenesis in posterofrontal cranial suture-derived mesenchymal cells in vitro, Plast Reconstr Surg 123(1) (2009) 31–43. [PubMed: 19116522]

[38]. Ellman MB, Yan D, Ahmadinia K, Chen D, An HS, Im HJ, Fibroblast growth factor control of cartilage homeostasis, J Cell Biochem 114(4) (2013) 735–42. [PubMed: 23060229]

[39]. Zhang K, Guo X, Zhao W, Niu G, Mo X, Fu Q, Application of Wnt Pathway Inhibitor Delivering Scaffold for Inhibiting Fibrosis in Urethra Strictures: In Vitro and in Vivo Study, Int J Mol Sci 16(11) (2015) 27659–76. [PubMed: 26610467]

[40]. Bian L, Hou C, Tous E, Rai R, Mauck RL, Burdick JA, The influence of hyaluronic acid hydrogel crosslinking density and macromolecular diffusivity on human MSC chondrogenesis and hypertrophy, Biomaterials 34(2) (2013) 413–421. [PubMed: 23084553]

[41]. Pelttari K, Winter A, Steck E, Goetzke K, Hennig T, Ochs BG, Aigner T, Richter W, Premature induction of hypertrophy during in vitro chondrogenesis of human mesenchymal stem cells correlates with calcification and vascular invasion after ectopic transplantation in SCID mice, Arthritis Rheum 54(10) (2006) 3254–66. [PubMed: 17009260]

[42]. Schramm C, Spitzer MS, Henke-Fahle S, Steinmetz G, Januschowski K, Heiduschka P, Geis-Gerstorfer J, Biedermann T, Bartz-Schmidt KU, Szurman P, The cross-linked biopolymer hyaluronic acid as an artificial vitreous substitute, Invest Ophthalmol Vis Sci 53(2) (2012) 613–21. [PubMed: 22199245]

[43]. Baier Leach J, Bivens KA, Patrick CW Jr., Schmidt CE, Photocrosslinked hyaluronic acid hydrogels: natural, biodegradable tissue engineering scaffolds, Biotechnol Bioeng 82(5) (2003) 578–89. [PubMed: 12652481]

[44]. Hellingman CA, Davidson ENB, Koevoet W, Vitters EL, Van Den Berg WB, Van Osch GJ, Van Der Kraan PM, Smad signaling determines chondrogenic differentiation of bone-marrow-derived mesenchymal stem cells: inhibition of Smad1/5/8P prevents terminal differentiation and calcification, Tissue engineering part A 17(7–8) (2011) 1157–1167. [PubMed: 21142619]

[45]. Chen G, Deng C, Li Y-P, TGF-β and BMP signaling in osteoblast differentiation and bone formation, International journal of biological sciences 8(2) (2012) 272. [PubMed: 22298955]

[46]. Dai F, Zhang F, Sun D, Zhang Z, Dong S, Xu J, CTLA4 enhances the osteogenic differentiation of allogeneic human mesenchymal stem cells in a model of immune activation, Brazilian Journal of Medical and Biological Research 48(7) (2015) 629–636. [PubMed: 26017342]

[47]. Li A, Xia X, Yeh J, Kua H, Liu H, Mishina Y, Hao A, Li B, PDGF-AA promotes osteogenic differentiation and migration of mesenchymal stem cell by down-regulating PDGFRα and derepressing BMP-Smad1/5/8 signaling, PLoS One 9(12) (2014) e113785. [PubMed: 25470749]

[48]. Lee K-S, Kim H-J, Li Q-L, Chi X-Z, Ueta C, Komori T, Wozney JM, Kim E-G, Choi J-Y, Ryoo H-M, Runx2 is a common target of transforming growth factor β1 and bone morphogenetic protein 2, and cooperation between Runx2 and Smad5 induces osteoblast-specific gene expression in the pluripotent mesenchymal precursor cell line C2C12, Molecular and cellular biology 20(23) (2000) 8783–8792. [PubMed: 11073979]

[49]. Coricor G, Serra R, TGF-beta regulates phosphorylation and stabilization of Sox9 protein in chondrocytes through p38 and Smad dependent mechanisms, Sci Rep 6 (2016) 38616. [PubMed: 27929080]

[50]. Faust D, Schmitt C, Oesch F, Oesch-Bartlomowicz B, Schreck I, Weiss C, Dietrich C, Differential p38-dependent signalling in response to cellular stress and mitogenic stimulation in fibroblasts, Cell Commun Signal 10 (2012) 6. [PubMed: 22404972]

[51]. Liu G, Vijayakumar S, Grumolato L, Arroyave R, Qiao H, Akiri G, Aaronson SA, Canonical Wnts function as potent regulators of osteogenesis by human mesenchymal stem cells, J Cell Biol 185(1) (2009) 67–75. [PubMed: 19349579]

[52]. Zhen X, Wei L, Wu Q, Zhang Y, Chen Q, Mitogen-activated protein kinase p38 mediates regulation of chondrocyte differentiation by parathyroid hormone, J Biol Chem 276(7) (2001) 4879–85. [PubMed: 11098049]

[53]. Mehlhorn A, Niemeyer P, Kaschte K, Muller L, Finkenzeller G, Hartl D, Sudkamp N, Schmal H, Differential effects of BMP-2 and TGF-β1 on chondrogenic differentiation of adipose derived stem cells, Cell proliferation 40(6) (2007) 809–823. [PubMed: 18021172]

[54]. Occhetta P, Pigeot S, Rasponi M, Dasen B, Mehrkens A, Ullrich T, Kramer I, Guth-Gundel S, Barbero A, Martin I, Developmentally inspired programming of adult human mesenchymal stromal cells toward stable chondrogenesis, Proceedings of the National Academy of Sciences 115(18) (2018) 4625–4630.

[55]. Feng Q, Lin S, Zhang K, Dong C, Wu T, Huang H, Yan X, Zhang L, Li G, Bian L, Sulfated hyaluronic acid hydrogels with retarded degradation and enhanced growth factor retention promote hMSC chondrogenesis and articular cartilage integrity with reduced hypertrophy, Acta Biomater 53 (2017) 329–342. [PubMed: 28193542]

[56]. Somoza RA, Correa D, Labat I, Sternberg H, Forrest ME, Khalil AM, West MD, Tesar P, Caplan AI, Transcriptome-Wide Analyses of Human Neonatal Articular Cartilage and Human Mesenchymal Stem Cell-Derived Cartilage Provide a New Molecular Target for Evaluating Engineered Cartilage, Tissue Eng Part A 24(3–4) (2018) 335–350. [PubMed: 28602122]

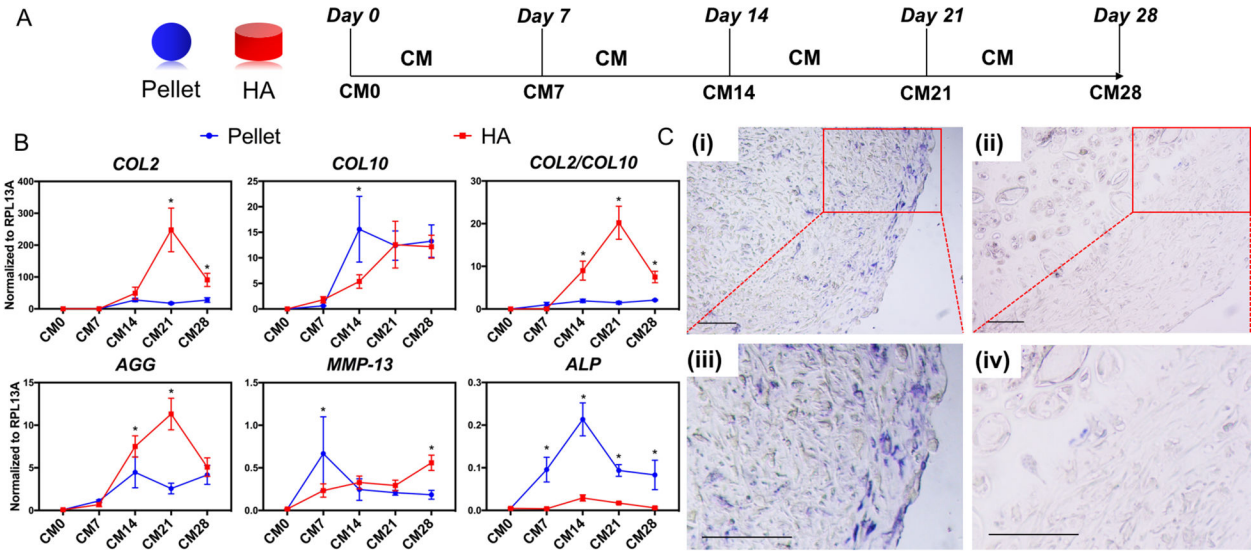

Figure 1.

(A) Schematic of control chondrogenesis experimental plan. MSC-formed pellets (Blue sphere) or MSC-laden HA constructs (red cylinder) were cultured in chondrogenic medium (CM) for up to 28 days. CM0, naïve MSC; CM7, 14, 21, and 28 represent samples cultured in CM for 7, 14, 21 and 28 days, respectively. **(B)** Real time-PCR analysis of gene expression profiles of chondrogenesis/hypertrophy markers in pellet cultures (blue line) and HA constructs (red line) of MSCs at different time points. All data were normalized to endogenous control ribosomal protein L13a (*RPL13A*). Values are presented as mean ± SD. N=4 per group. *=$p < 0.05$. **(C)** ALP staining (blue color) of CM21 pellet culture (i, iii) and CM21 HA culture (ii, iv) groups, showing prominent level of ALP activity. Scale bar=100μm.

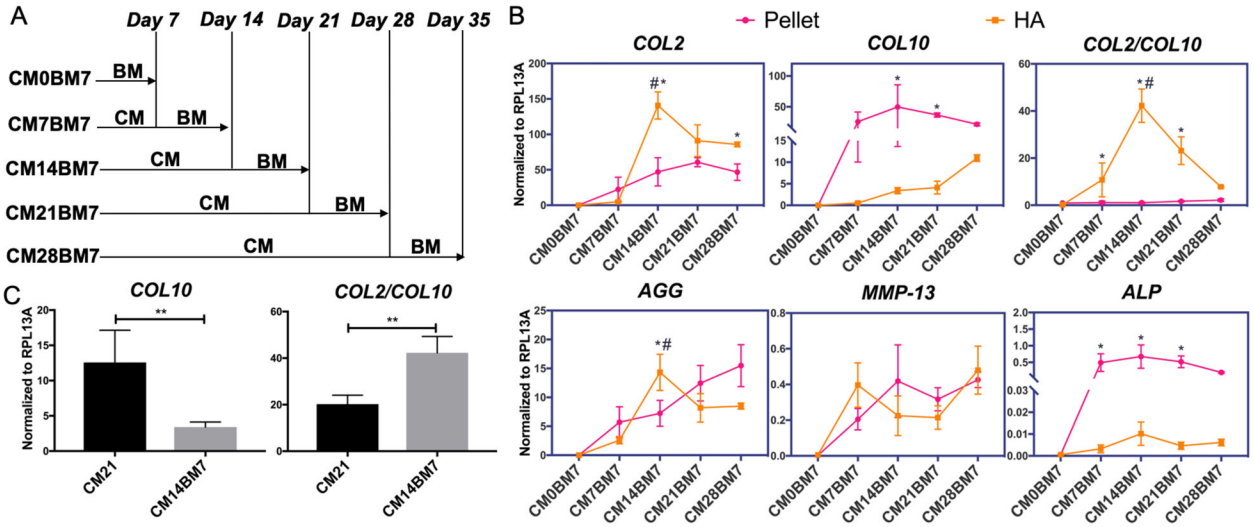

Figure 2.

(A) Schematic of modified chondrogenesis experimental plan. Pellet and HA hydrogel constructs of MSCs were cultured in CM for different time periods, followed by additional 7 days culture in basic medium (BM). CM0BM7, CM7BM7, CM14BM7, CM21BM7, and CM28BM7 represent, respectively, the samples being cultured in CM for 0, 7, 14, 21 or 28 days, plus additional 7 days culture in BM. **(B)** Real time-PCR analysis of gene expression profiles of chondrogenesis/hypertrophy markers in MSCs within pellet culture (pink line) and HA construct (orange line) at different time points. All data were normalized to *RPL13A*. Values are presented as mean ± SD (N = 4 per group). *, $p<0.05$, indicating significant difference between pellet and HA cultures in the CM14BM7 group. #, $p<0.05$, indicating significant difference between CM14BM7 and other groups in HA culture. **(C)** *COL10* gene expression levels and *COL2/COL10* gene expression ratios in the HA construct CM21 and CM14BM7 groups. CM14BM7 group displayed significantly lower *COL10* expression and higher ratio of *COL2/COL10*. All data were normalized to *RPL13A*. Values are presented as mean ± SD (N = 4 per group; **, $p<0.01$).

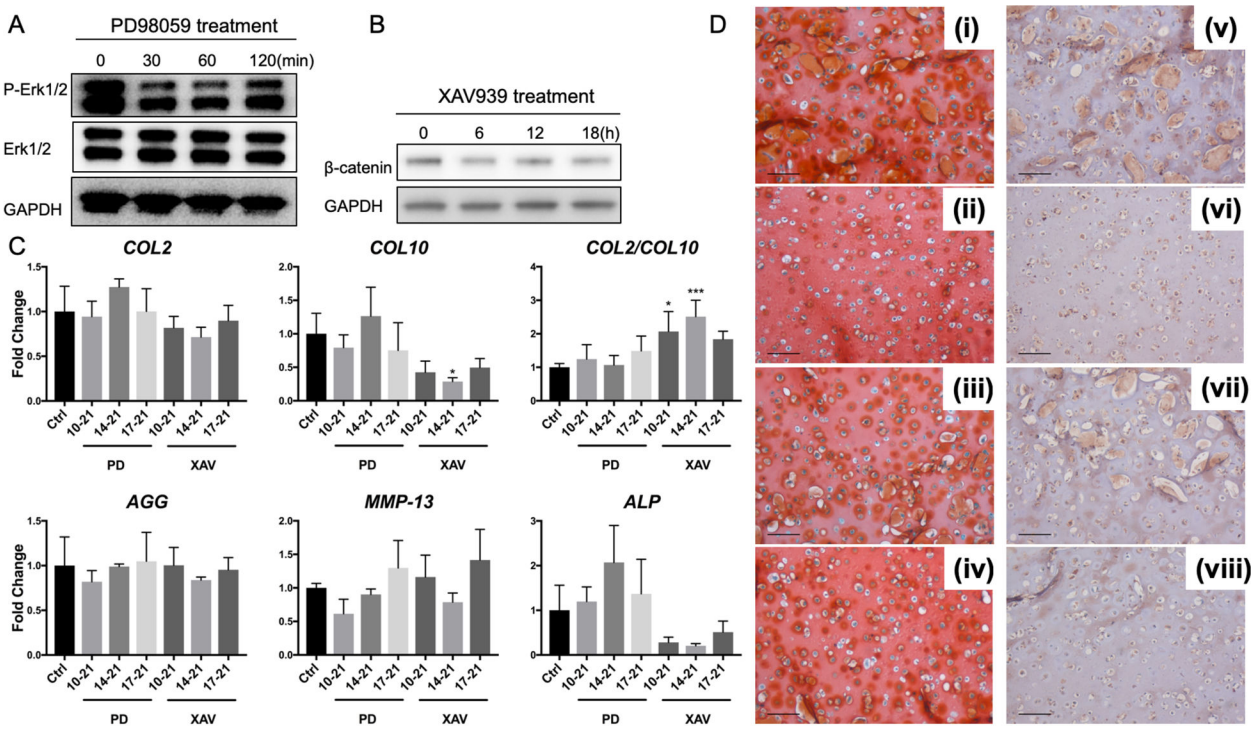

Figure 3.

Effect of PD98059 (PD) and XAV939 (XAV) treatment on gene expression of chondrogenesis and hypertrophy markers in CM14BM7 HA cultures. The efficacy of the two inhibitors was confirmed by Western blot analysis, showing that **(A)** level of phosphorylated Erk1/2 (P-Erk1/2) was reduced by PD treatment after 30 minutes, while **(B)** β-catenin level was reduced by XAV treatment after 6 hours. **(C)** Real time-PCR analysis of gene expression profiles of chondrogenesis/hypertrophy markers after PD and XAV treatment. CM14BM7 without treatment was set as control group (Ctrl). Results showed that PD treatment did not significantly change gene expression profiles, while XAV treatment downregulated *COL10* expression and upregulated the ratio of *COL2/COL10*. Values are presented as mean ± SD (N = 4 per group; *, $p<0.05$; ***, $p<0.001$). **(D)** Histology and immunohistochemistry of XAV939-treated groups. During 21-day culture of CM14BM7 HA constructs, XAV939 was added either from days 10 to 21 (ii, vi), or days 14 to 21 (iii, vii), or days 17 to 21 (iv, viii), with DMSO as the carrier control (i, v). Bar = 100 μm. Safranin O/Fast green staining (i-iv) showed no significant difference in GAG deposition. Collagen type X immunostaining (v-viii) showed that XAV939 treatment from days 10 to 21 displayed the lowest level of collagen type X deposition among all groups.

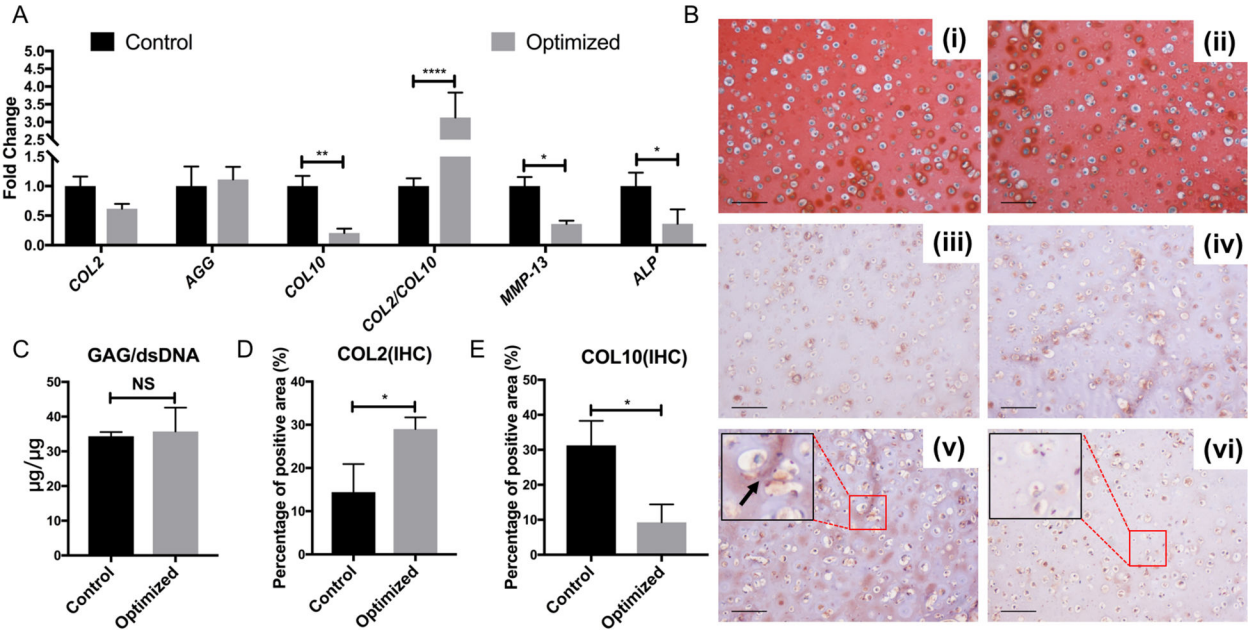

Figure 4.

Comparison of chondrogenesis and hypertrophy characteristics between Control (CM21 in HA) and Optimized (CM14BM7 in HA with XAV treatment from day 10–21) groups. **(A)** Gene expression profiling showed that the optimized group had lower gene expression of *COL10*, *MMP-13*, and *ALP*, and a higher ratio of *COL2/COL10*. Values are presented as mean ± SD (N = 4 per group; *, p<0.05; **, p<0.01; ****, p<0.0001). **(B)** Histology and immunohistochemistry analysis: Control (i, iii, v); Optimized (ii, iv, vi). Safranin O/Fast green staining (i, ii); collagen type II immunostaining (iii, iv); collagen type X immunostaining (v, vi). Bar = 100 μm. The Optimized group showed more intense collagen type II and less collagen type X (indicated by arrows) staining as quantified by image analysis shown in **(D)** and **(E)**, respectively. **(C)** GAG assay showed no significant difference between the two groups in term of GAG/DNA. Values are presented as mean ± SD (N = 3 per group; *, p < 0.05).

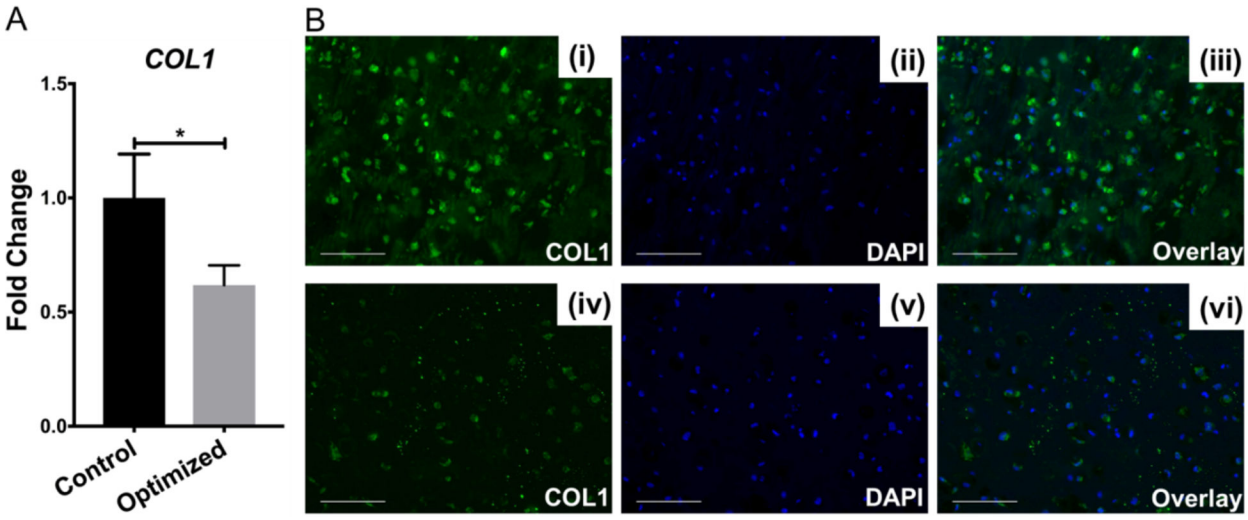

Figure 5.

Comparison of *COL1* gene expression in Control (CM21) and Optimized (CM14BM7 with XAV treatment on days 10–21) MSC HA constructs. **(A)** Reduced *COL1* was seen in Optimized group. Values are presented as mean ± SD (N = 4 per group; *, $p < 0.05$). **(B)** Collagen type I detection by immunofluorescence: Control group (i - iii); Optimized group (iv - vi). Less collagen type I deposition was seen in the Optimized group. Bar = 50 μm.

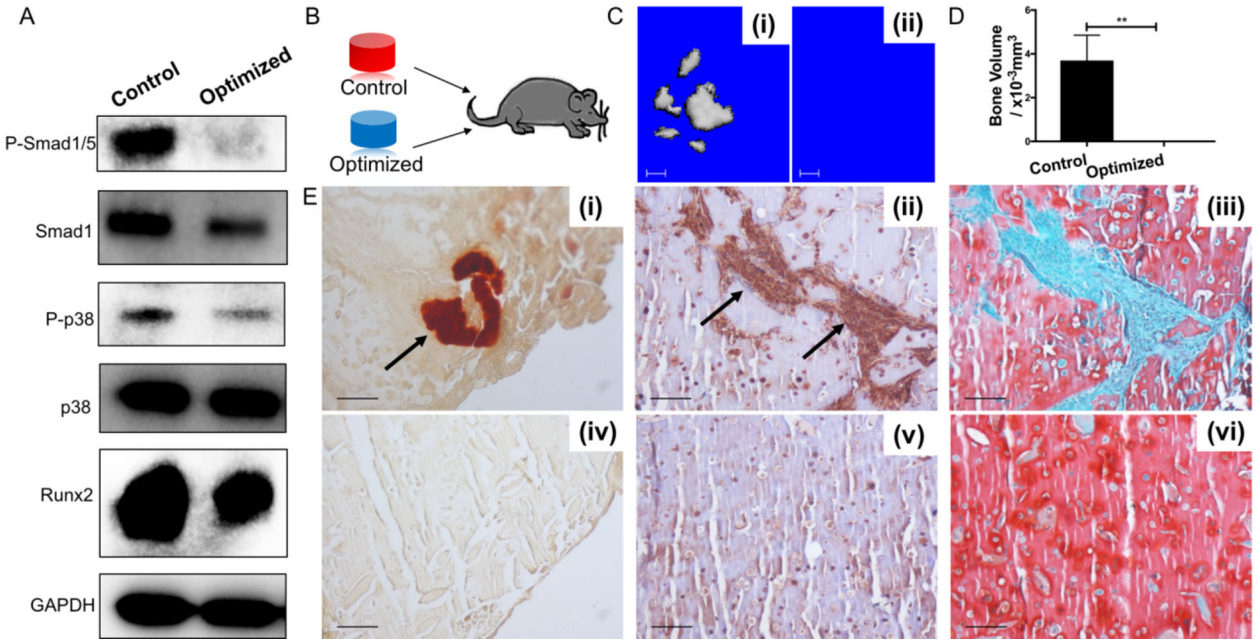

Figure 6.

Optimized group of HA chondrogenic constructs exhibits minimal osteogenic potential *in vitro* and *in vivo*. **(A)** Western blot of phosphorylated p38 (P-p38), p38, phosphorylated Smad1/5 (P-Smad1/5), Smad1, and Runx2 in the Control and Optimized groups. **(B)** Schematic of intramuscular transplantation into mice. **(C)** micro-CT analysis of bone formation *in vivo* for (i) Control group, and (ii) Optimized group. **(D)** Quantitation of bone volume in micro-CT analysis, with values presented as mean ± SD (N = 4 per group; *, $p < 0.05$). Bone formation was detected in the Control group but not in the Optimized group. **(E)** Histology and immunohistochemistry of Control (i, ii, iii) and Optimized (iv, v, vi) groups. (i, iv) Alizarin red staining; (ii, v) osteocalcin immunostaining; and (iii, vi) Safranin O/Fast green staining. Control group showed presence of calcification, osteocalcin deposition (indicated by black arrows), and less GAG deposition, compared to the Optimized group. Bar = 100 μm.

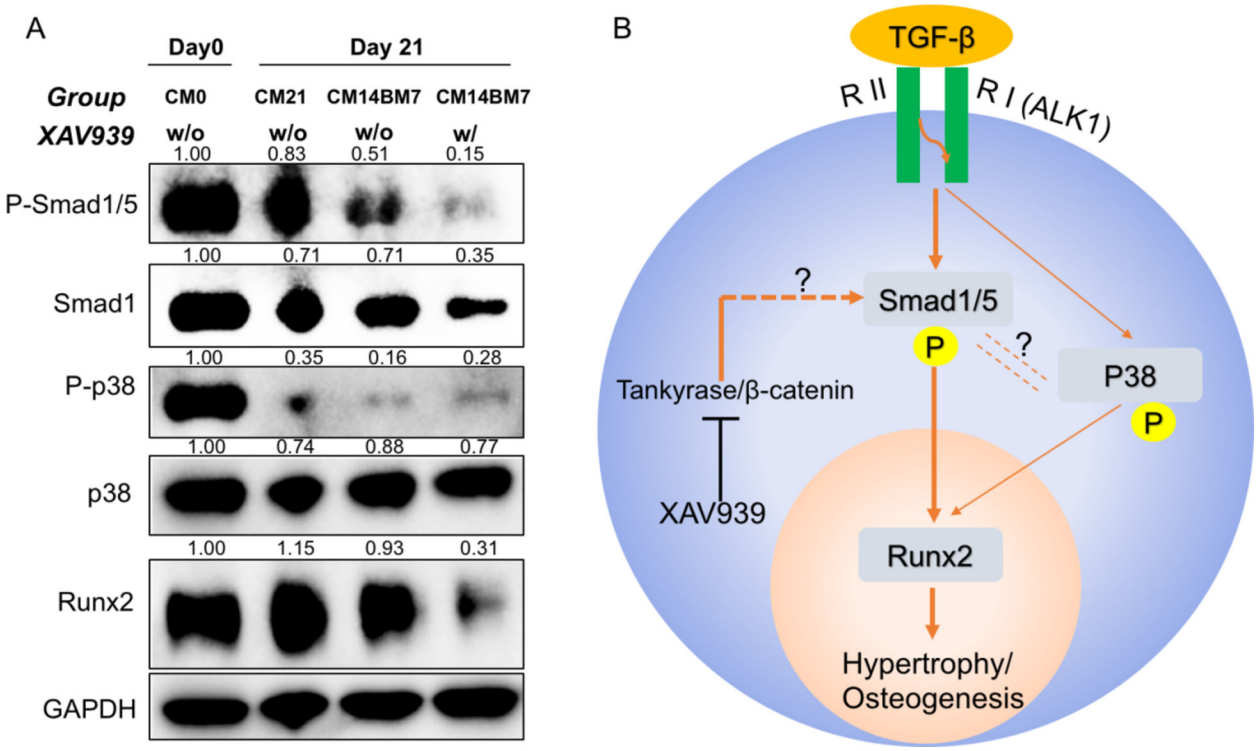

Figure 7.

XAV939 inhibition of hypertrophy/osteogenesis via modulation of TGF-β-Smad1/5-Runx2 signaling pathway. **(A)** Western blot of P-p38, p38, P-Smad1/5, Smad1, and Runx2 in naïve MSCs (CM0), Control group (CM21), and untreated (CM14BM7) and Optimized (CM14BM7 with XAV treatment on days 10–21) groups. Each band was first normalized to GAPDH, and then normalized to each CM0 group respectively. **(B)** Postulated regulatory pathways associated with hypertrophy/osteogenesis of MSCs undergoing chondrogenesis in 3D HA constructs, and potential mechanism of action underlying XAV939 treatment.